Magneto-optical rotation in atomic transitions between levels with $J=0$ and $J=1$

F. Schuller
Laboratoire de Physique des Lasers, UMR 7538 du CNRS, Université Paris-13, Avenue Jean-Baptiste Clément, 93430 Villetaneuse, France

D. N. Stacey
Clarendon Laboratory, Parks Road, Oxford OX1 3PU, United Kingdom
(Received 11 August 1998; revised manuscript received 12 April 1999)

We give a density-matrix account of an atom in a dilute vapor which is subject to a magnetic field and through which is propagating plane-polarized monochromatic light with frequency in the vicinity of a transition between levels of total angular momenta $J=0$ and 1, where the degeneracy may be in either the upper or lower level. The master equation approach allows saturation effects to be treated in a nonperturbative manner, and collisions are included within the context of the impact approximation. The particular case of the Voigt effect in a $(1\rightarrow 0)$ transition (lower level $J=1$) is considered in detail, and contrasted with that in $(0\rightarrow 1)$, already published; in the absence of collisions, the $(1\rightarrow 0)$ rotation spectrum is of Lorentzian form at all intensities, while if collisional relaxation is much faster than radiative decay, it takes the same form as for the $(0\rightarrow 1)$ case. The rotation produced by a magnetic field of arbitrary direction and the effects of atomic motion are also discussed. [S1050-2947(99)02108-3]

PACS number(s): 33.55.Ad, 33.55.Fi, 32.70.Jz

I. INTRODUCTION

The change in the state of polarization of light when traveling through a dilute gas subject to a magnetic field has been extensively studied, both experimentally and theoretically [1–9]. The simplest and most important case is when the light is plane polarized and propagates along the field direction (the Faraday or Macaluso-Corbino effect), but the Voigt effect, in which the magnetic field is perpendicular to the direction of propagation, has also been the subject of experiments. The main interest is when the frequency of the light is close to an atomic resonance. The development of tunable lasers gave the field renewed stimulus, leading notably to Faraday spectroscopy as a tool for the study of atomic structure and collisional effects; optical rotation can be studied as a function of frequency at constant field, or the laser can be tuned to the center of the atomic resonance and the variation of rotation recorded as a function of the magnetic field strength.

The theoretical description of the phenomena is in principle well understood; the basic equations which have to be solved are relatively straightforward, within the context of approximations which are generally justified in normal experimental conditions (for example, the impact treatment of atomic collisions). Unfortunately, the methods of solution generally employed involve further approximations which are not so widely applicable, thus giving results of limited use. This is particularly true with respect to saturation effects, which are very useful since they can produce sharp features in the rotation spectra directly associated with specific decay mechanisms; however, they have generally been treated perturbatively [10], despite the fact that with laser light it is easy to produce strong saturation effects. We have developed an approach using a master equation for the density matrix describing the system, which allows comparatively simple solutions for any strength of radiation field. This approach has previously been applied to the cases of atoms with $J_g=0$, $J_e=1$, where J_g, J_e are the ground and excited level total electronic angular momenta, respectively, with $J_g=1$, $J_e=0$ and with $J_g=\frac{1}{2}, J_e=\frac{1}{2}$. We refer to these as the $(0\rightarrow 1)$, $(1\rightarrow 0)$, and $(\frac{1}{2}\rightarrow\frac{1}{2})$ cases, respectively.

We have derived and solved the equations governing the Faraday effect for all three cases [11–13], and for the Voigt effect in the $(0\rightarrow 1)$ case [14]. The $(\frac{1}{2}\rightarrow\frac{1}{2})$ case, treated in [13], with degeneracy in both levels, differs fundamentally from the other two. However, the equations solved in [11,12,14] are special cases of equations which govern the response of atoms to plane-polarized light with its electric vector at any orientation to an applied magnetic field (and so are applicable to both the Voigt and Faraday effects and indeed intermediate geometries), and which are almost the same for the $(0\rightarrow 1)$ and $(1\rightarrow 0)$ cases. These equations are relatively simple, and readily solvable by computer for a given physical situation. We therefore give them explicitly in the present paper, and solve them to find the characteristics of the Voigt effect for the $(1\rightarrow 0)$ case, which has not been treated before. We contrast the results with those for the $(0\rightarrow 1)$ case; there are striking differences despite the similarity of the basic equations. It is useful to recall here the main features of the Faraday effect for the $(0\rightarrow 1)$ and $(1\rightarrow 0)$ cases, which were strikingly verified [15] by applying them to experimental data already in the literature [7]. In the $(0\rightarrow 1)$ case, the rotation spectrum is very straightforward at low intensities, but when saturation occurs there is competition between the two circular components of the polarization of the driving field for the ground-state population leading to observable effects over and above simple power broadening. Collisional relaxation of orientation and alignment is only important at high intensities. By contrast, in the $(1\rightarrow 0)$ case, whatever the strength of radiation field, there is no Faraday effect at all in the absence of relaxation processes which

redistribute atoms among the ground magnetic sublevels. This is because the atoms are optically pumped into the sublevel with $M_g=0$, a ''dark state'' from which they cannot be removed by absorption. This major difference between the $(0\rightarrow1)$ and $(1\rightarrow0)$ cases for the Faraday effect occurs despite the very similar equations which describe the two. The comparison of the Voigt effects is analogous to, but not identical with, that of the Faraday effects. It remains true that collisional relaxation of orientation and alignment is not important at low intensities in the $(0\rightarrow1)$ case. It is also true that optical pumping is significant even at vanishingly low intensities in the $(1\rightarrow0)$ case in the absence of collisions; however, for the Voigt geometry there is no dark state so the effect does not vanish.

As in our previous papers, we assume monochromatic incident light and a dilute gas. The $(0\rightarrow1)$ and $(1\rightarrow0)$ cases are developed in parallel, to highlight the contrast between the two. Calculations are carried out for stationary atoms, and atomic motion is taken into account subsequently by convolution. In the normal Voigt geometry, the plane of polarization of the incident light is at $\pi/4$ to the direction of the magnetic field, and the observed rotation is due to differential absorption of the polarization components along and perpendicular to the field. For this reason, the theory (in contrast to the Faraday effect) is valid only for rotations small compared with $\pi/4$. We first give the theory, then discuss the results.

II. OPTICAL BLOCH EQUATIONS

We use the definitions and nomenclature developed in [11–14]. A plane monochromatic wave is incident on a dilute sample of atoms of number density N. The wave is linearly polarized with electric vector $\mathbf{E}$ and its frequency ω is close to the atomic transition frequency ω_0. A constant magnetic field is applied to the system, with (for the Voigt geometry) its field vector $\mathbf{H}$ at right angles to the direction of propagation of the light. The angle θ between $\mathbf{E}$ and $\mathbf{H}$ will be set to $\pi/4$ to obtain explicit expressions for the Voigt effect, but in setting up the equations we maintain generality. Similarly, it is convenient to set up the density-matrix formalism to describe a system in which both levels can have nonzero angular momentum before specializing to the two cases of interest here.

The state of the system is described by a density matrix $\boldsymbol{\rho}$ with optical coherences ρ_{M_g,M_e} and Zeeman coherences $\rho_{M_g,M_g'}, \rho_{M_e,M_e'}$. A reduced stationary density matrix $\boldsymbol{\sigma}$ has been defined in [16] by introducing the following transformation:

$$\boldsymbol{\rho}(t)=\exp(-i\alpha t)\,\boldsymbol{\sigma}\exp(i\alpha t) \tag{1}$$

with

$$\alpha=\tfrac{1}{2}\omega(P_e-P_g), \tag{2}$$

where P_g and P_e are projection operators in the ground- and excited-state manifolds defined in the usual way by the expressions

$$P_g=\sum_{M_g}|M_g\rangle\langle M_g| \quad \text{and} \quad P_e=\sum_{M_e}|M_e\rangle\langle M_e|. \tag{3}$$

This transformation implies that we have for optical coherences the relation

$$\rho_{M_g,M_e}=\exp(i\omega t)\,\sigma_{M_g,M_e}, \tag{4}$$

whereas elements within one multiplet are not affected by the transformation.

With this procedure the following master equation for the reduced stationary density matrix $\boldsymbol{\sigma}$ has been derived from the Liouville equation [17]:

$$\frac{i}{\hbar}[H_m,\boldsymbol{\sigma}]+\frac{i}{\hbar}[V_{\text{eff}},\boldsymbol{\sigma}]+(\boldsymbol{\Phi}+\boldsymbol{\Gamma})\boldsymbol{\sigma}=0. \tag{5}$$

In this equation, H_m is a modified atomic Hamiltonian defined as

$$H_m=H_A-\frac{\hbar\omega}{2}(P_e-P_g) \tag{6}$$

with H_A the Hamiltonian of the atom in the static magnetic field. The second term on the right-hand side of this equation is the consequence of the removal of oscillations by the transformation (1). V_{eff}, which describes the interaction of the atom with the incident wave, is given by the expression

$$V_{\text{eff}}=-\tfrac{1}{2}P_e\boldsymbol{\mu}P_g\cdot\mathbf{E}-\tfrac{1}{2}P_g\boldsymbol{\mu}P_e\cdot\mathbf{E}, \tag{7}$$

where $\boldsymbol{\mu}$ is the atomic dipole operator.

Finally, the operators $\boldsymbol{\Phi},\boldsymbol{\Gamma}$ describe, respectively, collisional relaxation within the multiplets and natural (radiation) damping together with collisional relaxation of optical coherence. The effect of $\boldsymbol{\Phi}$ on each multiplet is most conveniently described in terms of an irreducible tensor basis T_{kq} for the density operator. Specializing now to the particular cases of interest, $\boldsymbol{\Phi}$ does not operate on a level with $J=0$, so we write for the part of the density operator within the $J=1$ manifold

$$\sigma_e=\sum_{k,q}\sigma_{kq}T_{kq} \quad \left(\sigma_g=\sum_{k,q}\sigma_{kq}T_{kq}\right), \tag{8}$$

where the first expression is appropriate to the $(0\rightarrow1)$ case, and the second, in large parentheses, to the $(1\rightarrow0)$ case. We shall maintain this convention in the following.

We then account for collisional destruction of orientation and alignment in the impact approximation by introducing relaxation rates f_k, $k=1,2$:

$$\boldsymbol{\Phi}T_{kq}=f_kT_{kq}, \tag{9}$$

where these rates are proportional to the number density of perturbing atoms.

The effect of $\boldsymbol{\Gamma}$ is given by

$$\boldsymbol{\Gamma}|M_e\rangle\langle M_e|=A|M_e\rangle\langle M_e|-A|g\rangle\langle g|,$$
$$\left(\boldsymbol{\Gamma}|e\rangle\langle e|=A|e\rangle\langle e|-\frac{A}{3}\sum_{M_g}|M_g\rangle\langle M_g|\right), \tag{10a}$$

$$\boldsymbol{\Gamma}|M_e\rangle\langle g| = \left(\frac{A}{2}+\gamma\right)|M_e\rangle\langle g|,$$

$$\left[\boldsymbol{\Gamma}|M_g\rangle\langle e| = \left(\frac{A}{2}+\gamma\right)|M_g\rangle\langle e|\right], \tag{10b}$$

where γ is the half-width at half maximum (HWHM) of the Lorentzian due to dephasing collisions and A is the Einstein coefficient for spontaneous emission for the transition.

We now define the Rabi frequency Ω_M in terms of the dipole matrix element by the relation

$$\hbar\Omega_M = \langle M|\boldsymbol{\mu}|g\rangle\cdot\mathbf{E} \quad (\hbar\Omega_M = \langle e|\boldsymbol{\mu}|M\rangle\cdot\mathbf{E}). \tag{11}$$

We further define an intensity as the product

$$I_M = \Omega_M\Omega_M^*. \tag{12}$$

According to this definition, one can show that for linearly polarized light I_M is given in terms of the field amplitude E and the angle θ between $\mathbf{E}$ and $\mathbf{H}$ by the relations

$$I_1 = I_{-1} = \frac{I}{2}\sin^2\theta, \tag{13a}$$

$$I_0 = I\cos^2\theta, \tag{13b}$$

where

$$I = \frac{1}{\hbar^2}|\boldsymbol{\mu}|^2E^2 \tag{14}$$

and

$$|\boldsymbol{\mu}|^2 \equiv |\langle J_e\|\boldsymbol{\mu}\|J_g\rangle|^2 \quad (|\boldsymbol{\mu}|^2 \equiv |\langle J_g\|\boldsymbol{\mu}\|J_e\rangle|^2),$$

the square of the reduced matrix element (as defined in [18]).

In our earlier work, we derived the optical Bloch equations for the quantities S_{gM}, where

$$s_{gM} = \Omega_M\sigma_{gM} \quad (s_{Me} = \Omega_M\sigma_{Me}). \tag{15}$$

For the present purposes, it is more convenient to introduce the combinations

$$s_{g1}+s_{g-1} = t_1+iu_t, \quad s_{g1}-s_{g-1} = t_2+iu_2,$$

$$s_{g0} = t_3+iu_3 \quad (s_{1e}+s_{-1e} = t_1+iu_1,$$

$$s_{1e}-s_{-1e} = t_2+iu_2, \quad s_{0e} = t_3+iu_3). \tag{16}$$

since these are more directly related to the Faraday and Voigt rotations (see Sec. III). The Bloch equations for the $(0\rightarrow 1)$ case then take the form

$$\left(R_2^r\frac{I_0}{2}+\Gamma\right)t_1 - R_2^rI_1t_3 - \Delta u_1 + \left(R_2^i\frac{I_0}{2}+\frac{\omega_c}{2}\right)u_2 = 0, \tag{17a}$$

$$\left(r^rI_1+R_1^r\frac{I_0}{2}+\Gamma\right)t_2 + \left(r^iI_1+R_1^i\frac{I_0}{2}+\frac{\omega_c}{2}\right)u_1 - \Delta u_2 + R_1^iI_1u_3 = 0, \tag{17b}$$

$$\Delta t_1 - \left(r^iI_1+R_1^i\frac{I_0}{2}+\frac{\omega_c}{2}\right)t_2 + \left[\left(\frac{4}{3A}+\frac{1}{6(A+f_2)}+r^r\right)I_1 + R_1^r\frac{I_0}{2}+\Gamma\right]u_1 + (4c+R_1^r)I_1u_3 = -I_1, \tag{17c}$$

$$-\left(R_2^i\frac{I_0}{2}+\frac{\omega_c}{2}\right)t_1 + \Delta t_2 + R_2^iI_1t_3 + \left(\frac{1}{2(A+f_1)}I_1 + R_2^r\frac{I_0}{2}+\Gamma\right)u_2 = 0, \tag{17d}$$

$$-R_2^r\frac{I_0}{2}t_1 + (R_2^rI_1+\Gamma)t_3 - R_2^i\frac{I_0}{2}u_2 - \Delta u_3 = 0, \tag{17e}$$

$$-R_1^i\frac{I_0}{2}t_2 + \Delta t_3 + (4c+R_1^r)\frac{I_0}{2}u_1 + (2dI_0+R_1^rI_1+\Gamma)u_3 = -\frac{I_0}{2}, \tag{17f}$$

where

$$c = 1/3A - 1/12(A+f_2), \tag{18a}$$

$$d = 1/3A + 1/6(A+f_2), \tag{18b}$$

$$\Gamma = A/2+\gamma, \tag{18c}$$

$$2R_1 = \frac{1}{i\omega_c/2+A+f_1}, \tag{19a}$$

$$2R_2 = \frac{1}{i\omega_c/2+A+f_2}, \tag{19b}$$

$$2r = \frac{1}{i\omega_c+A+f_2}, \tag{19c}$$

and where the superscripts indicate real and imaginary parts. ω_c is the positive frequency separation between the state with $M=-1$ and that with $M=+1$.

These equations have been applied previously to the $(0\rightarrow 1)$ Faraday and Voigt cases. In the Faraday geometry we set $I_0=0$, whereas in the usual Voigt geometry, i.e., with $\theta=\pi/4$, we have $I_0=2I_1$.

Equations (17) apply to the $(1\rightarrow 0)$ case provided the following modifications are made: (i) In the definitions of the variables t_i, u_i, the quantities s_{gM} are replaced by s_{Me}; (ii) ω_c is replaced by $-\omega_c$ throughout; (iii) on the right-hand side of Eqs. (17c) and (17f), I_1, I_0 are replaced by $I_1/3, I_0/3$; (iv) the quantity A is eliminated from the combinations $A+f_1, A+f_2$, so that the corresponding denominators now become proportional to f_1, f_2.

The first modification is an obvious redefinition, the second reflects the fact that the ordering of the Zeeman components of the line reverses if the lower level is split rather than the upper, while the third only leads to a scaling of all the t_i, u_i by a factor of 3. It can be simply understood by considering the special case of a weak radiation field and a magnetic field large enough to produce well-separated Zeeman components. If the laser is on resonance with one of these components, any atom can be excited if the lower level is

nondegenerate, whereas only one-third are in resonance if it is split. It is the fourth modification which reflects the major difference in the physics of the two cases. It expresses the fact that atoms cannot now leave the Zeeman sublevels by spontaneous emission, so that any nonequilibrium distribution of population among them caused by optical pumping will remain unless destroyed by collisional processes. Indeed, apart from the rescaling, the equations for the $(0 \rightarrow 1)$ and $(1 \rightarrow 0)$ cases are essentially the same if $f_1, f_2 \gg A$. This has implications for the interpretation of the solutions as discussed below.

Equations (17) can be solved by standard methods for linear equations, but given that there are only four nonzero coefficients in each it is convenient to proceed as follows: starting with (a),(d),(e), we express the variables t_2, u_1, u_3 as functions of t_1, t_3, u_2 and substitute these results into (b),(c),(f), which we solve numerically. Finally, we substitute these numerical solutions into (a),(d),(e) to obtain the values of t_2, u_1, u_3 required for determining the Faraday and the Voigt effects, respectively, as we now discuss.

III. VOIGT AND FARADAY ROTATION WITH STATIONARY ATOMS

A. Voigt and Faraday rotation angles

As has been shown in [11,14], the Faraday and Voigt rotation angles ψ_F, ψ_V for the $(0 \rightarrow 1)$ case are linked to the variables defined in Eq. (16) by the following relations:

$$\psi_F = -\frac{C}{I} t_2 x, \quad \psi_V = \frac{C}{I}(u_3 - u_1)x, \tag{20}$$

where x is the distance traveled through the medium and the constant C is given by

$$C = N|\boldsymbol{\mu}|^2 \frac{\omega}{\epsilon_0 c \hbar}. \tag{21}$$

These equations also apply to the $(1 \rightarrow 0)$ case. In the following, we disregard the factors C and x and consider only the quantity $(u_3 - u_1)/I$. We thus find that the basic equations (17) contain a description of the Faraday and Voigt effects in both the $(0 \rightarrow 1)$ and $(1 \rightarrow 0)$ cases. For the Faraday variables, the equations reduce to very simple analytical form [11]. This is because the radiation links the $J = 0$ level to only two of the $J = 1$ sublevels, and the intensity in the two circular components of the radiation is the same. Despite their greater complexity, however, the equations for the Voigt case are readily solvable as described in the preceding section. Since it is easy to obtain curves for any chosen values of the various parameters, we concentrate here on the situations which illustrate the important physical mechanisms, with particular emphasis on the comparison between the Voigt effect in the two cases. In the figures illustrating optical rotation, the curves are specified by values of $\omega_c, \gamma, f_1, f_2$, and the Rabi frequency, all expressed as fractions of the Einstein coefficient A for the transition, which sets a natural scale for the phenomena. The dimensionless quantity $A(u_3 - u_1)/I$ is then independent of the absolute value of A, and it is therefore convenient to use it as ordinate in the rotation spectra.

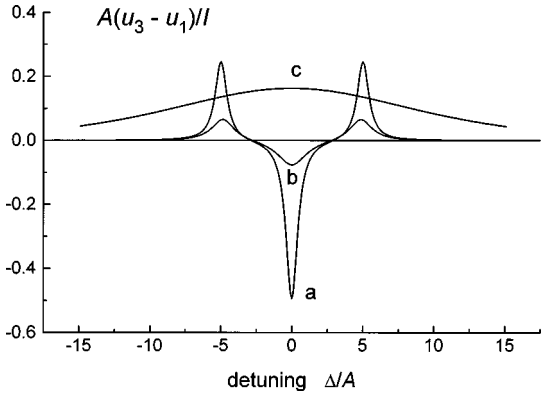

FIG. 1. Voigt effect in the $(0 \rightarrow 1)$ case with no collisions. The value of $A(u_3 - u_1)/I$, proportional to the Voigt rotation angle, is shown for $\omega_c/A = 10$, and intensities $I/A^2 = (\text{curve } a)\ 10^{-3}$, (curve *b*) 1, (curve *c*) 50, which correspond to weak, intermediate, and strong radiation fields. Case (c) is shown on a scale magnified by a factor of 100.

B. Voigt rotation with negligible collisional effects

We consider first the case $f_1 = f_2 = \gamma = 0$. A full discussion of the $(0 \rightarrow 1)$ case is given in [14], but we summarize the results here for the purposes of comparison. In a weak radiation field, the pattern is derivable from the familiar Zeeman triplet. The absorption in the central π component is twice that in the two σ components, leading to the profile shown in Fig. 1(a) (we take for the sake of clarity the case in which the triplet is well-resolved, i.e., ω_c significantly greater than A). As the intensity increases, there is a regime in which saturation affects each component individually, i.e., they still do not appreciably overlap; as a result, the rotation on resonance at each tends towards equality as in Fig. 1(b). Finally, at intensities such that the Rabi frequency is much greater than the Zeeman splitting, the individual components merge into a single broad feature, as in Fig. 1(c) [19].

The $(1 \rightarrow 0)$ case differs fundamentally from this because the splitting is in the lower rather than the upper level. Even with the weakest radiation fields, there is no relaxation mechanism to redistribute the atoms among the Zeeman sublevels, so in the stationary regime the population changes produced by optical pumping are not dissipated. The equilibrium populations of the sublevels depend on the Zeeman splitting and the intensity and frequency of the light, and one might thus anticipate a family of curves whose forms depend on these parameters in quite a complex way. However, the population decrease in a given state as the light is tuned towards it counterbalances the increase in atomic response in just such a way as to remove any features at the positions of the Zeeman components. One obtains a Lorentzian profile for all values of the parameters:

$$\frac{u_3 - u_1}{I} = \frac{A}{8} \frac{\omega_c^2}{\omega_c^2\left(5\Delta^2 + \frac{5}{4}A^2 + \omega_c^2 - \frac{I}{2}\right) + I^2}. \tag{22}$$

As the intensity is reduced, the full width at half maximum (FWHM) of this profile tends to the constant value $(A^2 + 4\omega_c^2/5)^{1/2}$; at high intensities, it increases as $(2/\sqrt{5})I/\omega_c$.

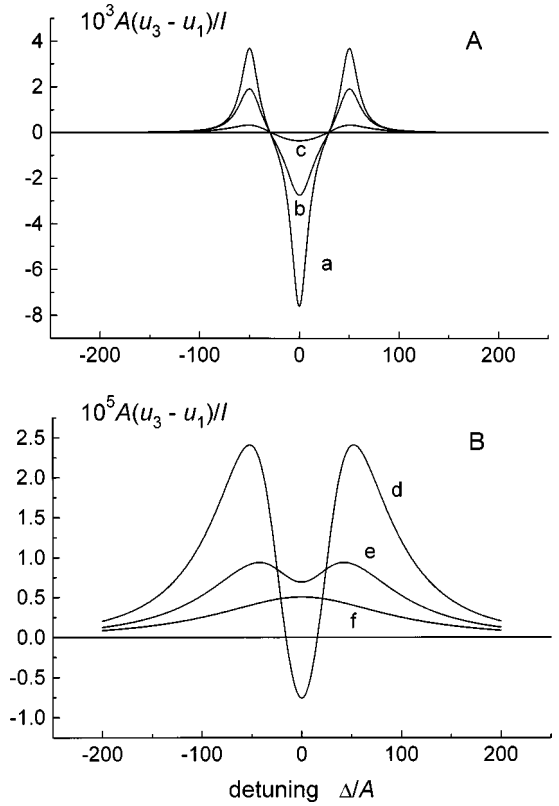

FIG. 2. Voigt effect in the $(1\rightarrow 0)$ case. The value of $A(u_3-u_1)/I$ is shown for $\omega_c/A=100$, collisional relaxation rates given by $\gamma/A, f_1/A, f_2/A=10$, and intensities $I/A^2=$(curve *a*) 10^{-3}, (curve *b*) 50, (curve *c*) 500, (curve *d*) 4×10^3, (curve *e*) 8×10^3, (curve *f*) 2×10^4. The curves in (a) show the onset of saturation, while those in (b) show saturation becoming complete. With this choice of parameters, collisional relaxation is much faster than the spontaneous emission rate, so the form of the curves applies also to the $(0\rightarrow1)$ case; however, the effect is then larger by a factor of 3 as explained in the text.

C. Voigt rotation with collisions

We now discuss the changes which occur when collisions play a significant role. Since we expect destruction of optical coherence due to collisions (represented by γ) and relaxation of orientation and alignment (f_1 and f_2, respectively) to be on comparable time scales [20], we set these three parameters equal for simplicity. The precise relationship between the different multipole relaxation rates is discussed in [20]. In the $(0\rightarrow1)$ case, phase-changing collisions do of course broaden the response curves of the individual components at all intensities, but f_1 and f_2 only affect the profile at intensities high enough for there to be a significant population in the excited level. By contrast, in the $(1\rightarrow0)$ case, they are of particular importance at the lowest intensities because they redistribute the populations of the ground level substates, tending to bring them back to equality. Consider the situation $f_1, f_2, \gamma \gg A \gg I^{1/2}$ shown in Fig. 2(a), curve *a*. Because the effects of optical pumping have been removed, one obtains essentially the same profile as that found for the weak radiation field effect in the $(0\rightarrow1)$ case, i.e., that shown in Fig. 1(a) but with the components broadened due to phase-changing collisions.

We now take the case where the Rabi frequency is not small compared with *A*, i.e., single atom saturation effects occur. We first assume that collisional relaxation still dominates both, and that the Zeeman splitting is large compared with the collisional broadening, i.e., we take $\omega_c \gg f_1, f_2, \gamma \gg A$. Now consider increasing *I*, starting at the low level discussed above, at which the peak rotation on the central component is twice that on either of the other two. Suppose the laser is tuned to one of the Zeeman components. It is then a good approximation to neglect stimulated transitions in the others, because they are well-resolved, so we have effectively a two-level system. As the intensity increases, the populations of the two levels connected by the laser light tend to equality; however, the populations of all three magnetic sublevels are tied together, so when saturation is complete the populations of all four states are $0.25N$. The depletion of the input beam under these circumstances is thus the same on all components, and independent of the incident intensity; it is simply set by the rate of spontaneous decay out of the upper level. The rotation on all three components thus tends to equality, just as in the $(0\rightarrow1)$ case, and the Voigt rotation, since it is proportional to the *fractional* differential absorption, decreases as $1/I$. This progression is shown in Fig. 2(a).

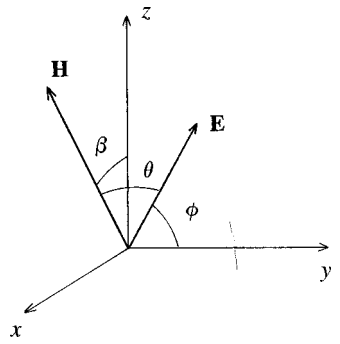

FIG. 3. Coordinate system used to describe the propagation of linearly polarized light for any direction of applied magnetic field. For key, see text.

Finally, we consider the profile when the intensity is so high that the stimulated transition rate is fast compared with all other processes, and the Rabi frequency is large compared with the Zeeman splitting. Then the width of the response curves is so large that the individual resonances are lost, and the profile has a single feature as in the $(0\rightarrow1)$ case shown in Fig. 1(c). This progression is shown in Fig. 2(b).

It is thus clear that when collisional effects dominate the natural decay rate, the $(0\rightarrow1)$ and $(1\rightarrow0)$ cases are very similar. This similarity is reflected in Eqs. (17) as mentioned earlier, i.e., the significant difference between the two cases, apart from the overall scaling factor of 3, is the elimination of *A* from the combinations $A+f_1, A+f_2$. If $A \ll f_1, f_2$, this is not a significant change under conditions such that u_1, u_3 are not too similar.

D. Arbitrary field orientation

In [21], we considered magneto-optical rotation for the $(0\rightarrow1)$ case when the direction of propagation makes an arbitrary angle with the direction of the magnetic field. Here we summarize the results and extend them, applying them also to the $(1\rightarrow0)$ case. Figure 3 shows a Cartesian frame in which the light propagates in the positive *x* direction. The

magnetic field is in the x,z plane at an angle β to the z direction. The electric vector, which is then located in the y,z plane, makes an angle ϕ with the y direction. Then θ (defined, as above, as the angle between **E** and **H**) is given by

$$\cos\theta = \sin\phi\cos\beta. \tag{23}$$

Following [21], we express the spherical components of the polarization **P** of the medium in terms of those of **E** using coefficients K_M as follows:

$$P_M = K_M E_M, \tag{24}$$

where M is defined, as usual, with respect to the magnetic field as quantization axis. We have that

$$K_M = -2|\boldsymbol{\mu}|^2 N \frac{s_{gM}}{I_M} \quad \left(K_M = -2|\boldsymbol{\mu}|^2 N \frac{s_{Me}}{I_M}\right) \tag{25}$$

so that the low-intensity form for the coefficients K_M is

$$K_M = |\boldsymbol{\mu}|^2 \frac{N}{\epsilon_0 \hbar} \frac{1}{\Delta - M\omega_c/2 - i\Gamma}$$

$$\left(K_M = |\boldsymbol{\mu}|^2 \frac{N}{3\epsilon_0 \hbar} \frac{1}{\Delta + M\omega_c/2 - i\Gamma}\right). \tag{26}$$

In [21], we introduced quantities $C_{MM'}$ defined by the relation

$$C_{MM'} = \sum_{M''} d_{M''M} K_{M''} d_{M''M'} \tag{27}$$

involving elements of the familiar rotation matrix $\mathbf{d}(\beta)$ associated with the rotation of the direction of **H** into that of the z axis of our Cartesian frame. We then showed that the magneto-optical rotation ψ is given by the following expression:

$$\psi = \frac{\omega x}{2c} \mathrm{Im}[\tfrac{1}{2}(R_1 - R_0)\sin 2\phi + Q], \tag{28}$$

where

$$R_1 = 1 + \frac{1}{\epsilon_0}(\tfrac{1}{2}C_{11} + \tfrac{1}{2}C_{-1-1} + C_{1-1}), \tag{29a}$$

$$R_0 = 1 + \frac{1}{\epsilon_0} C_{00}, \tag{29b}$$

$$Q = \frac{1}{\epsilon_0}\frac{i}{\sqrt{2}}(C_{10} + C_{-10}). \tag{29c}$$

From these expressions, the following explicit result is obtained:

$$\psi = \frac{\omega x}{4c}[\{\tfrac{1}{2}\,\mathrm{Im}(K_1 + K_{-1}) - \mathrm{Im}\,K_0\}\sin 2\phi\cos^2\beta + \mathrm{Re}(K_1 - K_{-1})\sin\beta]. \tag{30}$$

This was derived in [22] for the low-intensity limit in the $(0\rightarrow 1)$ case, i.e., with the K_M defined as in Eq. (26). Under these circumstances, the K_M have no angular dependence, and therefore, as pointed out in [22], the rotation is separable into Faraday and Voigt contributions. Equation (30) is in fact still valid in the nonlinear case. The separability of the two effects only holds in the linear regime, however, because otherwise the K_M depend on the angle θ which in turn depends on β and ϕ so that the optical rotation will vary in a nontrivial way with these angles.

To carry out explicit calculations, it is useful to express the rotation in terms of the variables defined in Eq. (15):

$$\psi = \frac{\omega x}{2\epsilon_0 \hbar c} N|\boldsymbol{\mu}|^2 \left[\left(\frac{u_3}{I_0} - \frac{u_1}{2I_1}\right)\sin 2\phi\cos^2\beta + \frac{t_2}{I_1}\sin\beta\right]. \tag{31}$$

From this expression, the magneto-optical rotation for either transition can be obtained at any angle and any intensity; the Voigt and Faraday effects appear as special cases.

IV. EFFECTS OF ATOMIC MOTION

The motion of the atoms leads to a distribution of central atomic frequencies due to the Doppler effect, giving for the case of thermal equilibrium the familiar Gaussian centered on ω_0. We define this distribution by its HWHM $\Delta\omega_D$. In the optically thin situation we are considering, the final rotation profiles are obtained by simple convolution of this Gaussian with the rotation spectra derived above. In Secs. III A–III C, we discuss the Voigt effect, while in Sec. IV D we compare the behavior of the Voigt and Faraday effects.

A. $(1\rightarrow 0)$ case without collisions

After convolution one obtains a Voigt profile for all intensities, since the spectrum for a stationary atom is of Lorentzian form. The area under the Lorentzian drops with increasing intensity, becoming $\sim 1/I$ for large I, so the largest effect is observed at line center at low intensity.

B. $(0\rightarrow 1)$ case without collisions

The stationary-atom spectrum has a peak rotation which drops with increasing intensity (Fig. 1). However, after convolution this ceases to be the case. The fact that the rotation produced by a single atom at low intensity averages to zero over frequency means that when convolved with a Doppler distribution of much greater width, the spectrum is strongly suppressed. When saturation effects become significant, the overall single-atom rotation is reduced, but it also becomes predominantly of one sign; at first, this is enough to cause the peak of the convolved curve to continue to grow. It ceases to do so, and eventually reduces, as the intensity increases further. This sequence is shown in Fig. 4.

C. $(1\rightarrow 0)$ case and $(0\rightarrow 1)$ case with collisions

We consider next the situation in which collisional relaxation dominates the natural decay rate, so that the $(1\rightarrow 0)$ and $(0\rightarrow 1)$ cases behave similarly. Qualitatively, the variation with intensity is as for the $(0\rightarrow 1)$ case without collisions, and for just the same reason: the convolved rotation

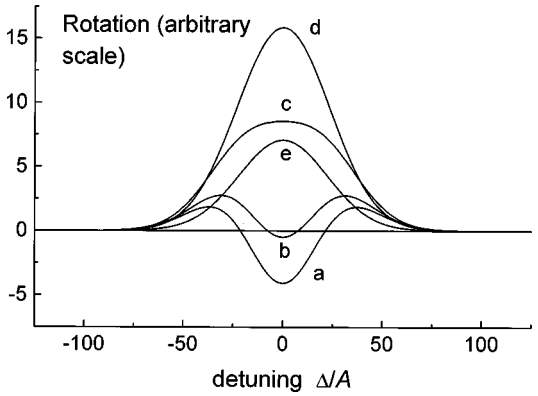

FIG. 4. Effect of inclusion of atomic motion on the Voigt effect. The example shown is for the $(0\rightarrow1)$ case without collisions, with $\omega_c/A=10$, convolved with a Gaussian function of HWHM $25A$. The intensity I/A^2 takes the following values: curve *a*, 10^{-3}; curve *b*, 0.1; curve *c*, 0.5; curve *d*, 10; curve *e*, 100. The largest rotation occurs when there is appreciable saturation present, in contrast to the case for stationary atoms. This is because the rotation averages to zero in weak radiation field.

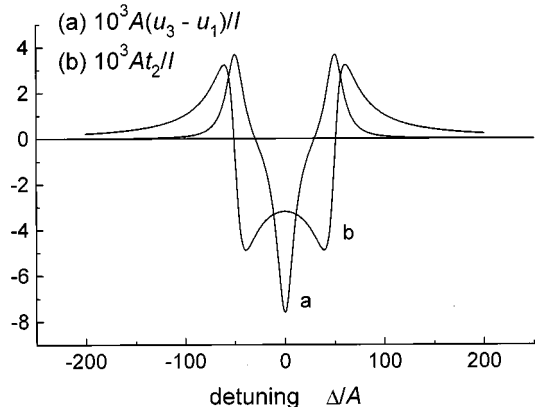

FIG. 5. Comparison of the Faraday and Voigt effects for the $(1\rightarrow0)$ case. The values of At_2/I (Faraday) and $A(u_3-u_1)/I$ (Voigt) are shown for $\omega_c/A=100$, collisional relaxation rates $\gamma/A, f_1/A, f_2/A=10$, and intensity $I/A^2=10^{-3}$. The two effects are comparable if as in this case ω_c is large enough for the components to be well-resolved.

spectrum at first increases with intensity because it ceases to average to zero when saturation effects become appreciable, reaches a maximum, and then steadily decreases.

D. Comparability with Faraday rotation

Since the Voigt effect for the $(1\rightarrow0)$ case without collisions depends so strongly on collisional effects, we first consider the more straightforward $(0\rightarrow1)$ case, at low intensity. As pointed out in [21], if the Zeeman splitting is larger than the radiation width, so that the triplet is well resolved, the peak Faraday and Voigt rotations are comparable. However, if the splitting is small compared with the linewidth, then the Voigt effect is smaller. In this regime, the magnitude of the Faraday effect is linear in the applied magnetic field, while the Voigt effect is quadratic. This is because the peak value of the Faraday rotation, which occurs at line center, is the difference between two dispersion curves which are displaced linearly with applied field. The Voigt rotation is the difference between a component which remains centered on ω_0 and the sum of two components, each of half the intensity of the first, centered at $\omega_0\pm\omega_c/2$.

These considerations carry over to the Doppler-broadened case; the Voigt effect is suppressed by comparison with the Faraday effect by an amount $\sim\omega_c/\Delta\omega_D$. It is evident that these results apply also at low intensity to the collision-broadened $(0\rightarrow1)$ case, and thus also to the $(1\rightarrow0)$ case provided that collisional relaxation is much faster than spontaneous emission. Figure 5 shows the $(1\rightarrow0)$ Faraday and Voigt rotations for the stationary atom case, while Fig. 6 shows the greater reduction in the latter caused by convolution. It is therefore much harder experimentally to study the Voigt effect without contamination with residual Faraday rotation than the converse.

V. VOIGT EFFECT AS A FUNCTION OF MAGNETIC FIELD

The rotation spectra discussed up to this point have all been given as a function of frequency, with the magnetic field kept constant in each case. This is because for the purposes of understanding the spectra in terms of physical mechanisms it is simplest to discuss the frequency response of stationary atoms, and then convolve in the Doppler distribution as a final step. However, experimentally it can be convenient to keep the frequency fixed near line center and measure the rotation as a function of magnetic field. This also has an advantage in that when the rotation is recorded as a function of frequency, Doppler broadening causes loss of detail and can limit the interpretation. When recorded as a function of field, however, saturation can cause narrow features (in the present case, associated with particular relaxation mechanisms) to appear in the spectra, even in the presence of atomic motion. Examples of experimental curves are given in [7] for the case of Faraday rotation, and their interpretation is discussed in [15].

We therefore give for completeness in Fig. 7 spectra as they would appear if recorded as a function of ω_c with the frequency of the radiation fixed near line center, supposing

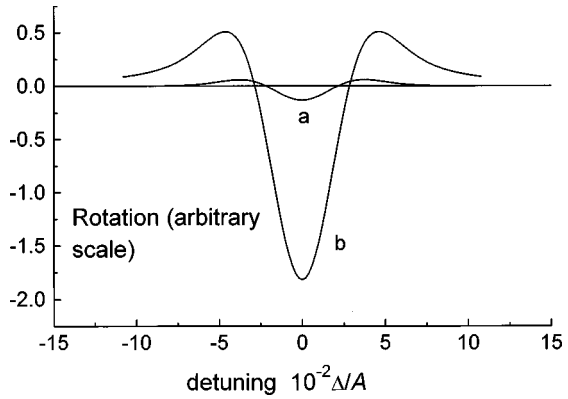

FIG. 6. Curve *a* Voigt and curve *b* Faraday rotation in weak radiation field for moving atoms in the $(1\rightarrow0)$ case, obtained by convolving the curves of Fig. 5 with a Gaussian function of HWHM $25A$. The value of ω_c is now much smaller than the linewidth, so the Voigt rotation is suppressed by comparison with that due to the Faraday effect.

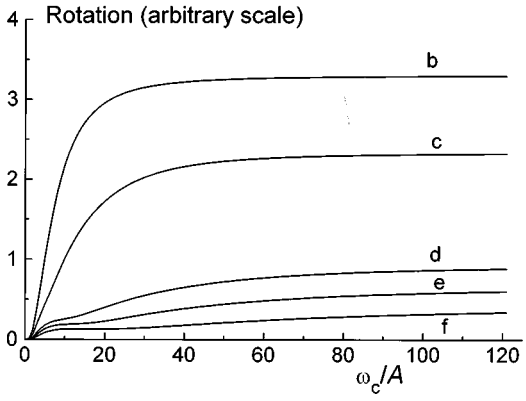

FIG. 7. Voigt rotation in the $(1\rightarrow 0)$ case, plotted as a function of ω_c/A with the frequency of the radiation fixed at a value near line center. The Doppler width of the transition is supposed large compared with the entire structure (see text). The curves correspond to the plots of Voigt rotation against frequency for fixed field in Fig. 2; values of the collisional relaxation are $\gamma/A, f_1/A, f_2/A = 10$ and the intensities are $I/A^2 = (\text{curve } b)\ 50$, (curve c) 500, (curve d) 4×10^3, (curve e) 8×10^3, (curve f) 2×10^4.

the transition to be Doppler-broadened. For ease of comparison, we choose the values of A, I, and the relaxation rates to be the same as those of the corresponding curves in Fig. 2; as explained earlier, this set of curves applies to both the $(0\rightarrow 1)$ and $(1\rightarrow 0)$ cases. In obtaining the curves shown in Fig. 7, it has been assumed throughout that the Doppler width of the transition is much larger than the entire structure [15]. The rotation for a given value of ω_c can then be found simply by integrating the frequency-dependent curve, since the Doppler distribution is effectively flat over the frequency range of interest. The rotation must always be zero for $\omega_c = 0$, and is symmetric about $\omega_c = 0$, so only the curves for positive ω_c are shown. The rotation tends to a constant value as ω_c increases; this is because once the magnetic field is large enough for the triplet to become resolved, no further changes can occur so long as $\omega_c \ll \Delta\omega_D$. When this ceases to be the case (beyond the region plotted in Fig. 7), our approximation that the Doppler width is much larger than the entire structure breaks down, and the rotation decreases asymptotically to zero.

No curve is shown corresponding to Fig. 2(a), since in the absence of saturation effects the average over frequency of the rotation produced by any given atom is zero. Hence, in the limit of very large Doppler width, the rotation is zero for all values of the field. The first effect of saturation appears in Fig. 7(b), the relative decrease in the response in the central component of the triplet apparent in Fig. 2(b) causing there to be a nonzero rotation which increases over a frequency range determined by the collisional rate since this governs the width of the individual atom response curve. The same general behavior is shown in Figs. 7(c)–7(f), the progressively slower rise to the maximum rotation occurring because the linewidth becomes dominated by the rapid rate of stimulated transitions, increasing as $\sqrt{I}$. A low-frequency feature associated with the collisional rates $(\gamma/A, f_1/A, f_2/A = 10)$ becomes discernible in Figs. 7(d)–7(f), but its exact shape and position depend also on the level of saturation.

VI. CONCLUSION

We have given the basic equations which govern the Faraday and Voigt rotations (and any combination of the two) for all radiation field strengths for the $(1\rightarrow 0)$ and $(0\rightarrow 1)$ cases. We have treated explicitly the Voigt effect for the $(1\rightarrow 0)$ case, contrasting it with the $(0\rightarrow 1)$ case. The major difference between the two occurs when there is negligible collisional relaxation, in which case optical pumping causes the $(1\rightarrow 0)$ rotation to become a simple Lorentzian function of frequency at all strengths of the radiation field. When collisional relaxation is more important than spontaneous emission, however, the two cases become very similar.

[1] W. Gawlik, J. Phys. B **12**, 3873 (1979).
[2] K. M. J. Tregidgo, P. E. G. Baird, M. J. D. Macpherson, C. W. P. Palmer, P. G. H. Sandars, D. N. Stacey, and R. C. Thompson, J. Phys. B **19**, 1143 (1986).
[3] Yu. V. Bogdanov, S. I. Kanorskii, I. I. Sobel'man, V. N. Sorokin, I. I. Struk, and E. A. Yukov, Opt. Spektrosk. **61**, 281 (1986) [Opt. Spectrosc. **61**, 446 (1986)].
[4] I. O. G. Davies, P. E. G. Baird, and J. L. Nicol, J. Phys. B **20**, 5371 (1987).
[5] K. H. Drake, W. Lange, and J. Mlynek, Opt. Commun. **66**, 315 (1988).
[6] M. G. Kozlov, Opt. Spektrosk. **67**, 1342 (1989) [Opt. Spectrosc. **67**, 789 (1989)].
[7] L. M. Barkov, D. A. Melik-Pashayev, and M. S. Zolotorev, Opt. Commun. **70**, 467 (1989).
[8] S. I. Kanorsky, A. Weis, J. Wurster, and T. W. Hänsch, Phys. Rev. A **47**, 1220 (1993).
[9] D. M. Lucas, R. B. Warrington, C. D. Thompson, and D. N. Stacey, J. Phys. B **27**, 5497 (1994).
[10] S. Giraud-Cotton, M. Giraud, and L. Klein, Chem. Phys. Lett. **32**, 317 (1975).
[11] F. Schuller, M. J. D. Macpherson, and D. N. Stacey, Physica C **147**, 321 (1987).
[12] F. Schuller, M. J. D. Macpherson, and D. N. Stacey, Opt. Commun. **71**, 61 (1989).
[13] F. Schuller, D. N. Stacey, R. B. Warrington, and K. P. Zetie, J. Phys. B **28**, 3783 (1995).
[14] F. Schuller, M. J. D. Macpherson, D. N. Stacey, R. B. Warrington, and K. P. Zetie, Opt. Commun. **86**, 123 (1991).
[15] K. P. Zetie, R. B. Warrington, M. J. D. Macpherson, D. N. Stacey, and F. Schuller, Opt. Commun. **91**, 210 (1992).
[16] G. Nienhuis, J. Phys. B **14**, 3117 (1981).
[17] F. Schuller and G. Nienhuis, Can. J. Phys. **62**, 183 (1984).
[18] M. E. Rose, *Elementary Theory of Angular Momentum* (Wiley, New York, 1957).
[19] It was stated in [14] that this curve is a Lorentzian. This is not

in fact the case, as can be seen from considering the behavior at large enough detuning for saturation effects to be negligible, in which case the rotation $\propto 1/\Delta^4$.

[20] F. Schuller and W. Behmenburg, Phys. Rep. **12C**, 153 (1974).

[21] F. Schuller, R. B. Warrington, K. P. Zetie, M. J. D. Macpherson, and D. N. Stacey, Opt. Commun. **93**, 169 (1992).

[22] N. H. Edwards, S. J. Phipp, and P. E. G. Baird, J. Phys. B **28**, 4041 (1995).